Regulation of eIF2α Phosphorylation by MAPKs Influences Polysome Stability and Protein Translation

Sana Parveen[1,#], Haripriya Parthasarathy[1,#], Dhiviya Vedagiri[1,2], Divya Gupta[1], Hitha Gopalan Nair[1], and Krishnan Harinivas Harshan[1,2]*

Affiliations: [1]CSIR-Centre for Cellular and Molecular Biology, Hyderabad-500007, India

[2]Academy of Scientific and Innovative Research (AcSIR), Ghaziabad-201002, India

[#]Equal Contributors

*Correspondence: hkrishnan@ccmb.res.in

Running title – MAPKs are central to protein translation regulation

Key words: Translation, p38 MAPK, ERK1/2, eIF2α, Mnk1/2, Polysome, Integrated stress response

ABSTRACT

Regulation of protein translation occurs primarily at the level of initiation and is mediated by multiple signaling pathways, majorly mechanistic target of rapamycin complex 1 (mTORC1), mitogen-activated protein kinases (MAPKs), and the eukaryotic translation initiation factor eIF2. While mTORC1 and eIF2α influence the polysome stability, MAPKs influence the phosphorylation of the cap-binding protein eIF4E and are known to influence translation of only a small set of mRNAs. Here, we demonstrate that p38 MAPK and ERK1/2 regulate translation through integrated stress response (ISR) pathways. Dual inhibition (dual-Mi) of p38 MAPK and ERK1/2 caused substantial phosphorylation of eIF2α in a synergistic manner, resulting in near-absolute collapse of polysomes. This regulation was independent of Mnk1/2, a well-studied mediator of translation regulation by the MAPKs. Dual-Mi-induced polysome dissociation was far more striking than that caused by sodium arsenite, a strong inducer of ISR. Interestingly, induction of ISR caused increased p38 phosphorylation, and its inhibition resulted in stronger polysome dissociation, indicating the importance of p38 in the translation activities. Thus, our studies demonstrate a major, unidentified role for ERK1/2 and more particularly p38 MAPK in the maintenance of homeostasis of polysome association and translation activities.

INTRODUCTION

Protein translation is a major regulatory event in gene expression in eukaryotes. Initiation is often the target for translation regulation and is achieved either by limiting the cap complex assembly or through preventing the recycling of pre-initiation complex (PIC) (1). Regulation is achieved through three major signal pathways, viz. mechanistic target of rapamycin complex 1 (mTORC1), initiation

52 factor eIF2 and MAPK-eIF4E pathways. While alterations in the activities of
53 mTORC1 and eIF2 directly impact polysome assembly, those in the eukaryotic
54 translation initiation factor (eIF4E) do not appear to be globally consequential. eIF4E,
55 the cap binding protein associates with eIF4G and eIF4A to form eIF4F complex
56 whose formation is influenced by eIF4E availability (2). eIF4E is phosphorylated at
57 S209 by MAPK interacting kinases Mnk1 and Mnk2 (3,4) that are regulated by two
58 mitogen activated protein kinases (MAPKs), viz. extracellular signal regulated
59 kinases (ERK1/2) and p38 MAPK (hereafter referred to as p38) (5,6). Even as the
60 role of phosphorylation on the affinity of eIF4E for the cap is contradicted (7),
61 phosphorylated eIF4E has transforming and oncogenic potentials (8-10). eIF4E
62 overexpression is reported in large cases of cancers (11). It is proposed that eIF4F
63 complex with phosphorylated eIF4E can translate certain transcripts that are
64 excluded by the complex with unphosphorylated eIF4E (9,12,13). eIF4E
65 phosphorylation was also well demonstrated to influence the translation of
66 specialised mRNAs including those of IκBα that mediates type I IFN production (14).

67 mTOR is a S/T kinase that assembles into one of the two distinct complexes
68 (mTORC1/mTORC2) (15,16). mTORC1 is a key regulatory hub for various cellular
69 and physiological activities such as translation and autophagy (17,18). mTORC1
70 regulates protein translation through at least two major substrates, eIF4E binding
71 protein (4EBP) and the ribosome S6 kinase, p70 S6K (19,20). mTORC1-mediated
72 multi-site phosphorylation of 4EBP1 releases eIF4E from sequestration facilitating its
73 availability for binding to 5’ caps of mature mRNAs. In spite of its perceivable key
74 role in translation, mTORC1 inhibition does not result in total inhibition of translation
75 activities (21-23). Studies in the past have identified several mRNAs that respond to
76 mTORC1 activity. mRNAs with a 5’ terminal oligopyrimidine (5’ TOP) element are

77 particularly vulnerable to translation inhibition caused by mTORC1 inhibitors such as
78 rapamycin, Torin1 and pp242 (21,22,24,25).

79 eIF2, a heterotrimeric complex formed by the association of α, β, and γ subunits, is a
80 critical component of the ternary complex with Met-tRNA^{Met} and GTP (eIF2-TC).
81 eIF2-TC binds to the 40S ribosome to form 43S PIC (26,27). Of these, eIF2α is the
82 regulatory subunit that upon phosphorylation at S52 leads to the inhibition of GDP
83 exchange with GTP after the hydrolysis of the bound GTP. eIF2α is phosphorylated
84 by integrated stress response (ISR) kinases HRI, GCN2, PKR, and PERK (26-28).
85 Of the known pathways, eIF2α phosphorylation has the most significant impact on
86 translation as this leads to the most severe translation inhibition (28).

87 Despite having their distinct spheres of regulation, there has not been any major
88 understanding on how these pathways influence each other under specific stimuli
89 barring a few reports (29). Certain degree of cross-activation of mTORC1 by ERK
90 through p90 ribosomal S6 kinase- mediated phosphorylation of RAPTOR is reported
91 (30). Partial dephosphorylation of eIF4E upon mTORC1 inhibition is also reported
92 (31). Studies also cite certain amount of cross-talk between mTORC1 and eIF2α
93 during autophagy (32). Interestingly, none of these pathways appear to wield a
94 dominant role over the other. A recent study in fact reported that about 90% of the
95 proteins affected by ISR induced by distinct signals are common barring a small
96 subset of unique proteins (29). This also suggests the existence of alternate
97 pathways to ensure basal translation activities under most of the conditions. Here,
98 we report that co-inhibition of p38 MAPK and ERK1/2 resulted in dose-dependent
99 phosphorylation of eIF2α indicative of ISR, strong dissociation of polysomes, and
100 inhibition of translation. Both cap-dependent and cap-independent pathways were
101 suppressed under these conditions. eIF2α phosphorylation by sodium arsenite

induced p38 MAPK, which was critical in maintaining basal translation activities. Mnk1/2 inhibition failed to bring about similar effects indicating the involvement of alternate pathways downstream of the MAPKs leading up to eIF2α phosphorylation. Interestingly, Mnk1/2 inhibition activated Akt that could possibly have contributed to the stabilization of translation activities under this condition. Our studies demonstrate a dominant role for p38 and ERK1/2 in the regulation of protein translation, through eIF2α phosphorylation.

Experimental procedures

Cell culture, inhibitors, and antibodies

All the cell lines were cultured in DMEM supplemented with 10% Fetal Bovine Serum, penicillin-streptomycin and NEAA. Sodium arsenite, U0126, p38 MAPK inhibitor VIII, Akt-1/2 inhibitor VIII, and ETP-45835 were procured from Merck Millipore and Torin1 was purchased from Tocris Bioscience. All the primary antibodies except β-Tubulin and GAPDH (Thermo Fisher Scientific) were purchased from Cell Signaling Technology. HRP-conjugated secondary antibodies were from Jackson ImmunoResearch.

Inhibitor treatments and immunoblotting

Cells were grown to 70-80% confluency, harvested, and lysed in NP-40 lysis buffer (33). Inhibitions were performed in most cases for 1- hour unless otherwise mentioned. Actively growing cells were treated with either vehicle or inhibitor-containing media before lysis. All the inhibitors were diluted in fresh DMEM right before the experiments. Protein concentration was estimated by BCA method (G Biosciences). Equal quantities of protein lysates were separated by SDS-PAGE,

transferred to an activated PVDF membrane, and immunoblotting was performed as mentioned elsewhere (33). β-Tubulin and GAPDH were used as loading controls.

Polysome preparation and profiling

Reagents for polysome analysis were purchased from Sigma and MP chemicals. Polysome profiles of the inhibited cells were analyzed as described earlier (33). Cells were grown in 150 cm^2 flasks till 70% confluency and inhibition studies were performed for 1- hour. Following the inhibition, the cells were harvested and washed twice with ice-cold 1×PBS containing 100 µg/mL cycloheximide. The lysates were prepared in polysome lysis buffer (20 mM Tris-Cl pH 8.0, 140 mM KCl, 1.5 mM $MgCl_2$, 0.5 mM DTT, 1% Triton X-100, 1× protease inhibitor, 0.5 mg/mL heparin, 100 µg/mL cycloheximide, 100 units of RNasin/mL) and crude RNA concentrations were spectrophotometrically measured. 175 µg of crude RNA lysates were layered on 11 mL of 10-50% linear sucrose gradients (20 mM Tris-Cl pH 8.0, 140 mM KCl, 1.5 mM $MgCl_2$, 0.5 mM DTT, 100 µg/mL cycloheximide, 10mM PMSF, and 10-50% sucrose) and the resulting gradients were centrifuged in SW-41 Ti rotor (Beckman Coulter) at 35,000 r.p.m. at 4°C for 3- hours. The samples were fractionated using Teledyne ISCO fraction collector system with a constant monitoring of absorbance at 254 nm to generate Polysome profiles.

Luciferase assay

Cells were seeded in 6 well plate format and grown till 70% confluency and the luciferase reporter plasmids were transfected using Lipofectamine 3000 (Thermo Fisher Scientific). One hour prior to harvesting, the transfected cells were treated with the specific inhibitors. Cells were harvested 10- hours post-transfection and the

148 luciferase reads were quantified using Dual-Luciferase reagents (Promega) as per
149 manufacturer's protocol on EnSpire multimode plate reader (Perkin Elmer).

150 **OPP Assay**

151 Total protein synthesis was quantified with the help of OPP-incorporation assay
152 based on Click-iT™ chemistry using the Click-iT™ Plus OPP-Alexa Fluor™ 488
153 protein synthesis assay kit (Life Technologies). The assay was carried out in
154 accordance with the manufacturer's recommendations. Briefly, Huh7.5 cells were
155 seeded in 8-well chamber slides (Lab-Tek) up to ~80% confluency, and
156 subsequently treated with either DMSO, p38 MAPK inhibitor VIII, U0126 or both for
157 1- hour. Post-treatment, the cells were treated with 20 µM OPP for 30 minutes at
158 37°C, followed by fixing with 3.7% formaldehyde and permeabilization with 0.5%
159 Triton X-100 in PBS. Click-iT reaction was carried out with Alexa Fluor 488-picolyl
160 azide for 30 minutes followed by nuclear staining using NuclearMask™ Blue stain.
161 Stained cells were imaged using AxioImager Z2 microscope using Alexa Fluor-488
162 and DAPI filters for detection. Threshold level was set using OPP-untreated cells.
163 Images were captured at 20× magnification. Image analysis was done using FIJI.
164 Mean whole-cell fluorescence of ~90 individual cells per sample from each set was
165 measured after background subtraction from individual fields. Data is represented as
166 mean fluorescence intensity.

167 **Cell viability assays**

168 Cell viability assays for treatments were carried out using MTT or trypan blue
169 exclusion assay. For all assays, cells were seeded till ~80% confluency and treated
170 with the pharmaceutical compound as mentioned. Vehicle- or inhibitor-treated cells
171 were trypsinized and mixed in 1:1 ratio with 0.4% trypan blue and counted using

Neubauer chamber to determine the cell count. For MTT assay, media containing MTT (final concentration of 0.5 mg/mL) was added to cells post treatment and incubated at 37°C for 3.5- hours. Formazan crystals formed were dissolved in 500 µL DMSO with mild agitation for 30 minutes. The assay readout was measured as absorbance at 440 nm, with a reference reading at 650 nm.

Statistical Analysis

Data from three independent experiments were used for statistical analysis using two-tailed Student's *t*-test for viability and dual-luciferase assays and represented graphically as Mean ± SEM. One-way ANOVA was used for OPP assay analysis and plotted as median with interquartile range. *, ** and *** indicate *p*-values < 0.05, 0.005 and 0.0005, respectively.

RESULTS

p38 MAPK and ERK1/2 dual inhibition inhibit eIF4E phosphorylation in a dose-dependent manner

p38 and ERK1/2, two major MAPKs regulate the phosphorylation of eIF4E through phosphorylating and activating Mnk1/2 (3,5,34,35). However, there is little mechanistic evidence on their synergistic regulation of eIF4E and subsequent impact on translation. We addressed this question by comparing eIF4E phosphorylation status under conditions of individual and simultaneous inhibitions of both MAPKs. First, we compared the degree of inhibition in Huh7.5 cells upon three combinations of p38 MAPK inhibitor VIII (p38i) and U0126 (ERK1/2i), viz. 12.5/25 µM, 25/50 µM and 50/100 µM concentrations. The status of eIF4E phosphorylation after 1- hour inhibition was analyzed as the measure of inhibition. A gradual and dose-dependent dephosphorylation of Mnk1 and eIF4E was observed and total dephosphorylation

was achieved at the combination of 50/100 µM concentrations (Figure 1A). However, cell viability was only modestly impacted by the treatments (Figure 1B). Total dephosphorylation of eIF4E was also achieved in MCF7 cells (Figure 1C). Next, we studied if the dual MAPK inhibition (dual-Mi) had any synergistic effect on eIF4E phosphorylation. Torin1, a potent mTOR inhibitor has been shown previously to affect translation. Torin1 treatment (750 nM) for 1- hour was done alongside MAPK inhibitions, to compare the effects of each treatment on MAPK substrate phosphorylation. Inhibition of mTORC1 was confirmed by the dephosphorylation of its substrates 4EBP1 and ULK1 (Figure 4A). As demonstrated in Figure 1D, the dual inhibition in Huh7.5 cells resulted in much stronger inhibition of Mnk1 and eIF4E than the individual inhibitions did, suggesting that p38 and ERK1/2 synergistically regulate eIF4E phosphorylation. No significant change was observed in the sample inhibited with Torin1, confirming the specificity of the treatments. Similar results were observed in MCF7 and HeLa cells (Figure S1 A & B, respectively)

Dual-Mi at high concentrations causes near-absolute collapse of polysomes and severe suppression of global translation

In order to characterize the effect of dual-Mi on global translation, polysome profiles in Huh7.5 cells treated with individual inhibitors or both (at 50/100 µM for p38 MAPK inhibitor VIII/U0126 respectively) were mapped. It may be noted that these concentrations were consciously chosen in this study so that the translation activities could be studied under conditions of complete inhibition of the MAPKs. Surprisingly, 1- hour dual-Mi in Huh7.5 cells caused near-absolute collapse of polysome peaks with corresponding accumulation of 80S, suggesting a global inhibition of translation activities (Figure 2A). No polysome peaks were visible under this condition, reminiscent of translation arrest caused by puromycin treatment (36). In comparison

221 to dual-Mi, individual inhibitions brought about only modest effects on the polysome
222 peaks (Figure 2B). The magnitude of polysome dissociation by dual-Mi was
223 remarkably higher than those caused by eIF2α phosphorylation by various methods
224 ((26,28) and Figure 6B) and mTORC1 inhibition by Torin1 (Figure 2C). Severe
225 impact of dual-Mi on polysome association was observed in MCF7 cells as well
226 (Figure S2A). Moderate collapse of polysomes was visible at a lower concentration
227 of 25/50 μM (Figure S2B), once again underlining the specificity of the response to
228 the inhibitions. The results demonstrated that the concurrent loss of activity of the
229 two MAPKs severely inhibits polysome assembly and possibly translation.

230 We next quantified the translation activities during dual-Mi in Huh7.5 cells by
231 labelling the nascent polypeptides using O-propargyl-puromycin (OPP) incorporation
232 assay. Cells were treated with p38 or ERK1/2 inhibitor or both of them for 1- hour
233 and were labeled with OPP for 30 minutes. Subsequently, they were analyzed by
234 fluorescence microscopy to quantify protein synthesis. As demonstrated in Figure
235 2D, appreciable fluorescence was detected throughout cytoplasm accompanied by
236 several bright foci in control cells indicating active translation. Both p38 and ERK1/2
237 inhibitions decreased the incorporation of OPP, evident from both lower intensity
238 fluorescence and reduced number of bright foci, implying lower translation rates. The
239 strongest inhibition of OPP incorporation was detected in dual-Mi treated cells
240 indicating very low levels of translation in them. Quantitative analysis of fluorescence
241 intensities revealed approximate intensity drop of 50% in samples treated with either
242 of the inhibitors and about 75% drop in dual-Mi samples, confirming strong inhibition
243 of translation activities in these cells (Figure 2E), substantiating the polysome
244 dissociation. These results also demonstrate that p38 and ERK1/2 are crucial
245 guardians of eukaryotic translation.

Mnk1/2 inhibition and eIF4E dephosphorylation do not recapitulate the polysome collapse caused by dual-Mi

Though Mnk1/2 double KO mice did not display any translation and growth defect, studies have demonstrated Mnk1/2 as key molecules in the phosphorylation of eIF4E (12). We studied if the effects on translation during dual-Mi are channelled through Mnk1/2. Mnk1/2 inhibitor ETP-45835 brought about eIF4E dephosphorylation in a dose-dependent manner (Figure 3A). In agreement with previous reports, polysome profiles of Mnk1/2 inhibited cells did not demonstrate any appreciable level of polysome dissociation (Figure 3B) in contrast to dual-Mi treatment (Figure 2A). These results indicate the participation of other signal pathways regulating polysome assembly and translation during dual-Mi treatment.

Dual-Mi causes moderate inhibition of mTORC1 activity

Since eIF4E dephosphorylation caused no significant impact on the polysome assembly, we studied the involvement of the other known pathways in coordinating the polysome dissociation by dual-Mi. mTORC1 pathway is a well-known regulator of translation and its inhibition causes significant depletion of polysomes and loss in translation activities ((22) and Figure 2C). We analyzed whether dual-Mi causes mTORC1 inhibition. Huh7.5 cells displayed moderate inhibition of mTORC1 activity, evident from the dephosphorylation of 4EBP1 and ULK1, two important substrates of mTORC1 (Figure 4A). Dose-dependence of the inhibition demonstrated the specificity of this observation (Figure 4B). Individually, ERK1/2 inhibition induced a stronger mTORC1 inhibition than p38 inhibition (Figure 4A). Torin1, an mTOR inhibitor, caused severe inhibition of mTORC1 activity. The degree of mTORC1 inactivation was less remarkable in MCF7 and HeLa cells (Figure S3 A & B,

respectively), indicating that this effect on mTORC1 activity is cell-specific and hence may not be contributing to the polysome dissociation by dual-Mi.

Dual-Mi induces strong eIF2α phosphorylation in a dose-dependent manner

Next, we tested the effect of dual-Mi on eIF2α phosphorylation. Huh7.5 cells subjected to dual-Mi were analyzed for the status of eIF2α phosphorylation. Individually, p38 inhibition caused a moderate eIF2α phosphorylation while ERK1/2 inhibition caused a stronger phosphorylation (Figure 5A). Interestingly, dual-Mi brought about a much stronger phosphorylation than the individual inhibitions, indicating that the two MAPKs regulate eIF2α independent of each other. These results also suggested that eIF2α phosphorylation through ISR could be a critical event behind the polysome dissociation during dual-Mi. A dose-dependent phosphorylation of eIF2α in response to varying concentrations of dual-Mi confirmed the specificity of the response (Figure 5B). eIF2α phosphorylation was consistently observed in MCF7 and HeLa cells as well (Figure S4 A & B respectively). Our results demonstrate that p38 and ERK1/2 are important players in the regulation of eIF2α phosphorylation and in the translation activities. Mnk1/2 inhibition could not recapitulate eIF2α phosphorylation (Figure 5C), ruling out its participation in the translation suppression associated with dual-Mi.

Activation of p38 upon stress is pivotal for the maintenance of low-level translation during eIF2α phosphorylation

The role of p38 as a key molecule facilitating stress response is well documented (37). We investigated the role of the two MAPKs in response to stress induced by general translation inhibitor sodium arsenite. Arsenite activates ISR kinases HRI, PKR, PERK and GCN that phosphorylate eIF2α (38-41). Treatment of Huh7.5 cells

with 40 µM arsenite induced strong eIF2α phosphorylation as expected. Interestingly, p38, but not ERK1/2 was phosphorylated by the treatments (Figure 6A), indicating its crucial role in the cell survival upon translation attenuation during ISR. Similar results were observed in MCF7cells (Figure 6A). Intriguingly, stress-induced p38 phosphorylation did not cause Mnk1/2 and eIF4E phosphorylation (Figure 6A), indicating the involvement of other mechanisms in the regulation of eIF4E phosphorylation by p38 under conditions that promote it. Sodium arsenite did not affect mTORC1 substrates in both Huh7.5 and MCF7 cells, ruling out the possibility of mTORC1 participating in ISR (Figure S5 A & B, respectively). Polysome analysis of arsenite treated cells showed a drop in translation as expected (Figure 6B). Despite a strong collapse of the heavy polysomes, lighter polysomes were intact. As indicated earlier, this polysome dissociation was less remarkable than that by dual-Mi, indicating the stronger translation inhibitory effects by the latter (Figures 2A & 6B).

Translation arrest is a general response to ISR and our results suggest that p38 activation is a probable feedback mechanism to sustain translation. In order to characterize the role of activated p38 upon ISR, we treated Huh7.5 cells with arsenite along with p38 inhibitor for 1- hour. This would, in principle, disallow the activation of p38 during ISR and hence could be an ideal set up to study the role of p38 in translation during ISR. Independently, p38 inhibition induced eIF2α phosphorylation similar in magnitude as arsenite did and their combined treatment did not further induce it (Figure 6C). Quite interestingly and as hypothesized, inhibition of p38 in cells treated with arsenite caused more severe polysome collapse as compared with arsenite treatment alone (Figure 6D). This result indicates that p38 activation is a crucial and remedial consequence to ISR in the maintenance of

minimal translation activity required for the synthesis of necessary proteins. Our results demonstrate that activation of p38 is crucial in sustenance of translation upon ISR induction.

Both cap-dependent and independent translations are inhibited by dual-Mi

Even though the default mode of translation is 5'-cap-dependent, cap-independent translation is promoted under several physiological conditions of stress (42). Even under eIF2α phosphorylation mediated translational arrest, a set of mRNAs are translated actively. To verify whether dual-Mi suppresses cap-independent translation, we used a bicistronic luciferase assay where translation of *Renilla* luciferase (Rluc) is cap-dependent whereas that of firefly luciferase (Fluc) is driven by HCV or EMCV IRES (Figure 7A) (43). Cells transfected with either of these vectors were subjected to dual-Mi and translation efficiencies were measured through luciferase activities. Interestingly, both Fluc and Rluc activities from HCV IRES construct were inhibited by approximately 60% after 1- hour of inhibition, indicating that dual-Mi mediated translation arrest inhibits both cap-dependent and cap-independent translation (Figure 7B). Inhibitions of similar magnitude from EMCV IRES construct confirmed the above observation (Figure 7C). A conventional analysis based on F/R ratio would not identify these inhibitions as both cap-dependent and independent translations were impacted similarly. These results are in agreement with the severe translation arrest described in previous section and indicate that concurrent inhibition of p38 and ERK1/2 affects translation machinery as a whole.

eIF2α phosphorylation is reversed during long-term dual-Mi

The profound loss in polysome assembly and translation inhibition during dual-Mi for 1- hour did not appear to affect the cellular viability. Long-term dual-Mi significantly inhibited cell viability as anticipated (Figure 8A), but, a considerable population of cells remained active at the end of the treatment. We investigated if the ISR is reversed during the long-term dual-Mi (24- hours) in Huh7.5 cells. eIF4E remained inhibited throughout the inhibition period, confirming the sustained inhibition of the MAPKs (Figure 8B). Interestingly, eIF2α remained phosphorylated until 12- hours post treatment and subsequently returned to the basal levels (Figure 8B), indicating that the ISR was reversed by 24- hours. Since Akt is an important regulator in cell survival (44), we studied its phosphorylation. The surviving cells indeed displayed higher phosphorylation of Akt from 4- hours of treatment onwards and gradually increased until 24- hours (Figure 8C). These results demonstrate that despite a severe inhibition of translation activities by dual-Mi, a significant fraction of the cells recover from this inhibition over a period time and we speculate that Akt could be an important player in this survival.

Mnk1/2 inhibition promotes Akt phosphorylation

While investigating the potential mechanism of activation of Akt phosphorylation during the prolonged dual-Mi, we noticed that Mnk1/2 inhibition for 1- hour resulted in higher S473 Akt phosphorylation in a dose-dependent manner (Figure 8D) indicating that Mnk1/2 inhibition is inducing mTORC2. As in the case of Mnk1/2 (Figure 5C), the concurrent inhibitions of Akt and Mnk1/2 failed to make any change in the phosphorylation status of eIF2α (Figure 8E), ruling out the involvement of Akt during

dual-Mi. However, it is compelling to suggest that Akt phosphorylation during prolonged dual-Mi could be important in the survival of the cells.

DISCUSSION

Being a complex process, translation is often studied from single-pathway perspectives. Recent advancements in RNA deep sequencing and ribosome profiling has revolutionized the field by enabling identification of the transcripts that are regulated by distinct signal pathways at multiple stages of the process. However, the cross talks between major pathways involved in the translation regulation need deeper understanding. A recent comprehensive report explained cross-talk between mTORC1 and eIF2α pathways (29). Another report suggests that upon DNA damage, mTORC1 may regulate eIF2α phosphorylation via PERK and GCN2, to promote cell migration (45). Yet another study proposes that HRI-mediated ISR may inhibit mTORC1 activity in the liver to mitigate ineffective erythropoiesis (46). In these contexts, our study reveals a central role of p38 and ERK1/2, two MAPKs that have been shown to influence translation initiation by phosphorylating eIF4E. Our study identifies a novel mechanism of regulation where p38 and ERK1/2 regulate eIF2α phosphorylation and hence ISR. The impact of dual inhibition was profound and achieved near-total polysome dissociation that is not detected in any other individual conditions including mTOR inhibition and eIF2α phosphorylation by known agents. Clearly, the two molecules synergistically regulated eIF2α. Even as this study has not identified the specific kinase that mediates eIF2α phosphorylation, it helps in characterizing a major mechanism that has not been reported before.

Our studies underline the importance of p38 in maintaining the translation homeostasis upon stress (47). p38, but not ERK1/2, was activated upon arsenite

391 treatment, indicating that the former is important in conditions of ISR. Interestingly,
392 p38 phosphorylation did not lead to eIF4E phosphorylation suggesting the
393 requirement of other factors in the regulation of the cap-binding protein. Additionally,
394 ERK1/2 inhibition caused more noticeable dephosphorylation of eIF4E in all cell lines
395 tested, implying the stronger influence by this MAPK. Although p38 activation upon
396 arsenite treatment has been documented previously (48,49), our interests were to
397 investigate its role in maintenance of translation under conditions of arsenite toxicity.
398 Treatment of cells with arsenite and p38i simultaneously revealed a further depletion
399 of polysomes, lending additional proof to its activation status under conditions of
400 arsenite stress. Interestingly,

401 The most studied target of the two MAPKs in translation regulation is Mnk1/2.
402 Previous studies have looked very closely at the role of Mnk1/2 and eIF4E
403 phosphorylation in translation and their impact on global translation was less than
404 appealing (50,51). Neither Mnk1/2 double knockout nor specific inhibitors have
405 identified any significant impact on polysome assembly (12,52). Our studies using
406 Mnk1/2 inhibitor are in total agreement with this. Importantly, Mnk1/2 inhibition did
407 not bring about eIF2α phosphorylation unlike dual-Mi did, thereby excluding its
408 participation in the mechanism we describe. It would be interesting to characterize
409 the involvement of the other known downstream targets of MAPKs, RSK and
410 MAPKAPKs under similar conditions.

411 Despite playing a major role, eIF2α phosphorylation alone cannot be implicated in
412 the magnitude of translation arrest by dual-Mi. That is because eIF2α
413 phosphorylation by various agents does not trigger such collapse in polysome
414 assembly as in dual-Mi as demonstrated by our study and others (38,53,54). Thus
415 dual-Mi appears to involve additional pathways and enforce a consolidated effect on

translation. mTORC1 does not appear to be a key player in this as it was not inhibited consistently across cell types during dual-Mi.

We considered whether Akt phosphorylation upon Mnk1/2 inhibition protects eIF2α from phosphorylation. However dual inhibition of Mnk1/2 and Akt failed to notice any change. Interestingly, dual-Mi prevented Akt phosphorylation for long duration further strengthening the possibility of Akt phosphorylation in the process. However, appearance of phospho-Akt from 4- hours onwards indicated its possible role in the diminishing effects of dual-Mi and revival of the cells. As an upstream effector of the mTOR pathway that senses nutrient and oxygen deprivation and as a pro-survival signal, activation of Akt is an intriguing observation that suggests a possible feedback mechanism that initiates at later time points in dual-Mi.

Specificity and universal appeal of our findings were strengthened by the consistency of the observations across three distinct cell lines. The original objective of this study was to investigate the impact of total dephosphorylation of eIF4E on the polysome association and hence we consciously chose higher concentrations of MAPK inhibitors. eIF2α phosphorylation, the key finding in this study, was induced even at lower concentrations of inhibitors and followed a dose-dependency indicating the specificity of their effect. In addition, the cell viability was only moderate at 1-hour inhibition when most of our studies were performed.

Dual-Mi had prolonged effect on eIF2α phosphorylation. The inhibitors caused phosphorylation as long as 12- hours indicating that feedback mechanisms to neutralize ISR were not effective. One major question is how the cells are able to sustain without crashing during a severe translational repression. Quite clearly, a set of proteins critical for survival were being translated despite very low translation

activities. It would be interesting to identify such proteins and the mechanisms that allow their translation. Activation of cap-independent mechanism is quite well accepted under conditions of translation suppression by mTORC1 inhibition (55). However, since dual-Mi caused severe suppression of cap-independent translation as well, the translating proteins are less likely to use this mode of translation. ERK1/2 activation promotes cell survival and proliferation in response to growth stimuli by driving the expression of pro-survival proteins. Response of p38 to stress stimuli depends more on the kinetics of its activation and can thus be either pro-survival or pro-apoptotic (56). Comparing our long duration dual-Mi observations to current understandings of MAPK signalling, it is possible that this cross-talk between MAPKs in general is allowing cells to remain viable despite seemingly negligible amounts of translation in the presence of high levels of eIF2α phosphorylation.

All MAPKs are known to respond to ER-stress in a myriad of ways, from transcriptionally upregulating pro-survival molecules, to stemming apoptotic signals, and seem to behave differently in different cell lines. p38 activation during ER-stress has been shown to cause switch from autophagy to apoptosis, mediated by PERK and eIF2α (57). MEK-ERK signalling has also been shown to be necessary for combating amino-acid deprivation in hepatocytes through GCN2 activation (58). These studies primarily see MAPK activation as a response to ISR that help combat the stress. Our studies also demonstrate that p38 is critical in the basal translation activities during stress. However, we also demonstrate that inhibition of these MAPKs can cause severe ISR. From our studies, p38 appears to be more critical to the balance in translation activities. Though inhibition of either of the two MAPKs caused eIF2α phosphorylation, only p38, not ERK1/2, was activated upon ISR induction. Since p38 inhibition causes ISR and eIF2α phosphorylation, we speculate

that the subsequent feedback phosphorylation of p38 could be critical in limiting the ISR and stabilizing translation. Thus p38 seems to be a critical molecule in the post-ISR rescue of translation activities. Additionally, p38 could also be critical in maintaining the low translation activities during ISR.

Author contributions

S.P., H.P., and K.H.H., conceived the study. S.P., H.P., D.V., D.G., and H.G.N performed the experiments. S.P., H.P., and K.H.H., analyzed the results. K.H.H wrote the manuscript while S.P., and H.P., edited it.

Acknowledgement

We thank Rupesh Balaji for assisting in polysome profiling. Special thanks to Mohan Singh for logistical assistance for several experiments. HCV-IRES and EMCV-IRES constructs were kind gifts from Dr. Saumitra Das.

Funding

This work was supported by funding from Department of Biotechnology, Govt. of India (BT/PR21356/MED/30/1779/2016). S.P, H.P and D.G received fellowships from Council of Scientific and Industrial Research, Govt. of India.

REFERENCES

1. Gebauer, F., and Hentze, M. W. (2004) Molecular mechanisms of translational control. *Nature reviews. Molecular cell biology* **5**, 827-835
2. Duncan, R., Milburn, S. C., and Hershey, J. W. (1987) Regulated phosphorylation and low abundance of HeLa cell initiation factor eIF-4F suggest a role in translational control. Heat shock effects on eIF-4F. *The Journal of biological chemistry* **262**, 380-388
3. Pyronnet, S., Imataka, H., Gingras, A. C., Fukunaga, R., Hunter, T., and Sonenberg, N. (1999) Human eukaryotic translation initiation factor 4G (eIF4G) recruits mnk1 to phosphorylate eIF4E. *The EMBO journal* **18**, 270-279
4. Joshi, B., Cai, A. L., Keiper, B. D., Minich, W. B., Mendez, R., Beach, C. M., Stepinski, J., Stolarski, R., Darzynkiewicz, E., and Rhoads, R. E. (1995) Phosphorylation of eukaryotic protein synthesis initiation factor 4E at Ser-209. *The Journal of biological chemistry* **270**, 14597-14603
5. Waskiewicz, A. J., Flynn, A., Proud, C. G., and Cooper, J. A. (1997) Mitogen-activated protein kinases activate the serine/threonine kinases Mnk1 and Mnk2. *The EMBO journal* **16**, 1909-1920

6. Morley, S. J. (1997) Intracellular signalling pathways regulating initiation factor eIF4E phosphorylation during the activation of cell growth. *Biochemical Society transactions* **25**, 503-509
7. Scheper, G. C., and Proud, C. G. (2002) Does phosphorylation of the cap-binding protein eIF4E play a role in translation initiation? *European journal of biochemistry* **269**, 5350-5359
8. Lazaris-Karatzas, A., Montine, K. S., and Sonenberg, N. (1990) Malignant transformation by a eukaryotic initiation factor subunit that binds to mRNA 5' cap. *Nature* **345**, 544-547
9. Furic, L., Rong, L., Larsson, O., Koumakpayi, I. H., Yoshida, K., Brueschke, A., Petroulakis, E., Robichaud, N., Pollak, M., Gaboury, L. A., Pandolfi, P. P., Saad, F., and Sonenberg, N. (2010) eIF4E phosphorylation promotes tumorigenesis and is associated with prostate cancer progression. *Proceedings of the National Academy of Sciences of the United States of America* **107**, 14134-14139
10. Topisirovic, I., Ruiz-Gutierrez, M., and Borden, K. L. (2004) Phosphorylation of the eukaryotic translation initiation factor eIF4E contributes to its transformation and mRNA transport activities. *Cancer research* **64**, 8639-8642
11. Carroll, M., and Borden, K. L. (2013) The oncogene eIF4E: using biochemical insights to target cancer. *J Interferon Cytokine Res* **33**, 227-238
12. Ueda, T., Watanabe-Fukunaga, R., Fukuyama, H., Nagata, S., and Fukunaga, R. (2004) Mnk2 and Mnk1 are essential for constitutive and inducible phosphorylation of eukaryotic initiation factor 4E but not for cell growth or development. *Mol Cell Biol* **24**, 6539-6549
13. Siddiqui, N., and Sonenberg, N. (2015) Signalling to eIF4E in cancer. *Biochemical Society transactions* **43**, 763-772
14. Herdy, B., Jaramillo, M., Svitkin, Y. V., Rosenfeld, A. B., Kobayashi, M., Walsh, D., Alain, T., Sean, P., Robichaud, N., Topisirovic, I., Furic, L., Dowling, R. J. O., Sylvestre, A., Rong, L., Colina, R., Costa-Mattioli, M., Fritz, J. H., Olivier, M., Brown, E., Mohr, I., and Sonenberg, N. (2012) Translational control of the activation of transcription factor NF-kappaB and production of type I interferon by phosphorylation of the translation factor eIF4E. *Nat Immunol* **13**, 543-550
15. Brown, E. J., Albers, M. W., Shin, T. B., Ichikawa, K., Keith, C. T., Lane, W. S., and Schreiber, S. L. (1994) A mammalian protein targeted by G1-arresting rapamycin-receptor complex. *Nature* **369**, 756-758
16. Sabatini, D. M., Erdjument-Bromage, H., Lui, M., Tempst, P., and Snyder, S. H. (1994) RAFT1: a mammalian protein that binds to FKBP12 in a rapamycin-dependent fashion and is homologous to yeast TORs. *Cell* **78**, 35-43
17. Saxton, R. A., and Sabatini, D. M. (2017) mTOR Signaling in Growth, Metabolism, and Disease. *Cell* **168**, 960-976
18. Wullschleger, S., Loewith, R., and Hall, M. N. (2006) TOR signaling in growth and metabolism. *Cell* **124**, 471-484
19. Hay, N., and Sonenberg, N. (2004) Upstream and downstream of mTOR. *Genes & development* **18**, 1926-1945
20. Wang, X., and Proud, C. G. (2011) mTORC1 signaling: what we still don't know. *Journal of molecular cell biology* **3**, 206-220
21. Jefferies, H. B., Reinhard, C., Kozma, S. C., and Thomas, G. (1994) Rapamycin selectively represses translation of the "polypyrimidine tract" mRNA family. *Proceedings of the National Academy of Sciences of the United States of America* **91**, 4441-4445
22. Thoreen, C. C., Chantranupong, L., Keys, H. R., Wang, T., Gray, N. S., and Sabatini, D. M. (2012) A unifying model for mTORC1-mediated regulation of mRNA translation. *Nature* **485**, 109-113
23. Hsieh, A. C., Costa, M., Zollo, O., Davis, C., Feldman, M. E., Testa, J. R., Meyuhas, O., Shokat, K. M., and Ruggero, D. (2010) Genetic dissection of the oncogenic mTOR pathway reveals druggable addiction to translational control via 4EBP-eIF4E. *Cancer cell* **17**, 249-261

24. Thoreen, C. C., Kang, S. A., Chang, J. W., Liu, Q., Zhang, J., Gao, Y., Reichling, L. J., Sim, T., Sabatini, D. M., and Gray, N. S. (2009) An ATP-competitive mammalian target of rapamycin inhibitor reveals rapamycin-resistant functions of mTORC1. *The Journal of biological chemistry* **284**, 8023-8032
25. Hsieh, A. C., Liu, Y., Edlind, M. P., Ingolia, N. T., Janes, M. R., Sher, A., Shi, E. Y., Stumpf, C. R., Christensen, C., Bonham, M. J., Wang, S., Ren, P., Martin, M., Jessen, K., Feldman, M. E., Weissman, J. S., Shokat, K. M., Rommel, C., and Ruggero, D. (2012) The translational landscape of mTOR signalling steers cancer initiation and metastasis. *Nature* **485**, 55-61
26. Hinnebusch, A. G. (2014) The scanning mechanism of eukaryotic translation initiation. *Annual review of biochemistry* **83**, 779-812
27. Jackson, R. J., Hellen, C. U., and Pestova, T. V. (2010) The mechanism of eukaryotic translation initiation and principles of its regulation. *Nature reviews. Molecular cell biology* **11**, 113-127
28. Andreev, D. E., O'Connor, P. B., Fahey, C., Kenny, E. M., Terenin, I. M., Dmitriev, S. E., Cormican, P., Morris, D. W., Shatsky, I. N., and Baranov, P. V. (2015) Translation of 5' leaders is pervasive in genes resistant to eIF2 repression. *eLife* **4**, e03971
29. Klann, K., Tascher, G., and Munch, C. (2020) Functional Translatome Proteomics Reveal Converging and Dose-Dependent Regulation by mTORC1 and eIF2alpha. *Mol Cell* **77**, 913-925 e914
30. Carriere, A., Romeo, Y., Acosta-Jaquez, H. A., Moreau, J., Bonneil, E., Thibault, P., Fingar, D. C., and Roux, P. P. (2011) ERK1/2 phosphorylate Raptor to promote Ras-dependent activation of mTOR complex 1 (mTORC1). *The Journal of biological chemistry* **286**, 567-577
31. Joubert, P. E., Stapleford, K., Guivel-Benhassine, F., Vignuzzi, M., Schwartz, O., and Albert, M. L. (2015) Inhibition of mTORC1 Enhances the Translation of Chikungunya Proteins via the Activation of the MnK/eIF4E Pathway. *PLoS pathogens* **11**, e1005091
32. Wengrod, J. C., and Gardner, L. B. (2015) Cellular adaptation to nutrient deprivation: crosstalk between the mTORC1 and eIF2alpha signaling pathways and implications for autophagy. *Cell Cycle* **14**, 2571-2577
33. George, A., Panda, S., Kudmulwar, D., Chhatbar, S. P., Nayak, S. C., and Krishnan, H. H. (2012) Hepatitis C virus NS5A binds to the mRNA cap-binding eukaryotic translation initiation 4F (eIF4F) complex and up-regulates host translation initiation machinery through eIF4E-binding protein 1 inactivation. *The Journal of biological chemistry* **287**, 5042-5058
34. Wang, X., Flynn, A., Waskiewicz, A. J., Webb, B. L., Vries, R. G., Baines, I. A., Cooper, J. A., and Proud, C. G. (1998) The phosphorylation of eukaryotic initiation factor eIF4E in response to phorbol esters, cell stresses, and cytokines is mediated by distinct MAP kinase pathways. *The Journal of biological chemistry* **273**, 9373-9377
35. Waskiewicz, A. J., Johnson, J. C., Penn, B., Mahalingam, M., Kimball, S. R., and Cooper, J. A. (1999) Phosphorylation of the cap-binding protein eukaryotic translation initiation factor 4E by protein kinase Mnk1 in vivo. *Mol Cell Biol* **19**, 1871-1880
36. Blobel, G., and Sabatini, D. (1971) Dissociation of mammalian polyribosomes into subunits by puromycin. *Proceedings of the National Academy of Sciences of the United States of America* **68**, 390-394
37. Whitmarsh, A. J. (2010) A central role for p38 MAPK in the early transcriptional response to stress. *BMC Biol* **8**, 47
38. McEwen, E., Kedersha, N., Song, B., Scheuner, D., Gilks, N., Han, A., Chen, J. J., Anderson, P., and Kaufman, R. J. (2005) Heme-regulated inhibitor kinase-mediated phosphorylation of eukaryotic translation initiation factor 2 inhibits translation, induces stress granule formation, and mediates survival upon arsenite exposure. *The Journal of biological chemistry* **280**, 16925-16933
39. Brostrom, C. O., Prostko, C. R., Kaufman, R. J., and Brostrom, M. A. (1996) Inhibition of translational initiation by activators of the glucose-regulated stress protein and heat shock

protein stress response systems. Role of the interferon-inducible double-stranded RNA-activated eukaryotic initiation factor 2alpha kinase. *The Journal of biological chemistry* **271**, 24995-25002

40. Sun, H., Yang, Y., Shao, H., Sun, W., Gu, M., Wang, H., Jiang, L., Qu, L., Sun, D., and Gao, Y. (2017) Sodium Arsenite-Induced Learning and Memory Impairment Is Associated with Endoplasmic Reticulum Stress-Mediated Apoptosis in Rat Hippocampus. *Frontiers in Molecular Neuroscience* **10**
41. Taniuchi, S., Miyake, M., Tsugawa, K., Oyadomari, M., and Oyadomari, S. (2016) Integrated stress response of vertebrates is regulated by four eIF2α kinases. *Scientific reports* **6**, 32886
42. Holcik, M., and Sonenberg, N. (2005) Translational control in stress and apoptosis. *Nature reviews. Molecular cell biology* **6**, 318-327
43. Pudi, R., Srinivasan, P., and Das, S. (2004) La protein binding at the GCAC site near the initiator AUG facilitates the ribosomal assembly on the hepatitis C virus RNA to influence internal ribosome entry site-mediated translation. *The Journal of biological chemistry* **279**, 29879-29888
44. Hemmings, B. A., and Restuccia, D. F. (2012) PI3K-PKB/Akt pathway. *Cold Spring Harbor perspectives in biology* **4**, a011189
45. Harvey, R. F., Poyry, T. A. A., Stoneley, M., and Willis, A. E. (2019) Signaling from mTOR to eIF2alpha mediates cell migration in response to the chemotherapeutic doxorubicin. *Sci Signal* **12**
46. Zhang, S., Macias-Garcia, A., Velazquez, J., Paltrinieri, E., Kaufman, R. J., and Chen, J. J. (2018) HRI coordinates translation by eIF2αP and mTORC1 to mitigate ineffective erythropoiesis in mice during iron deficiency. *Blood* **131**, 450-461
47. Akkari, L., Gregoire, D., Floc'h, N., Moreau, M., Hernandez, C., Simonin, Y., Rosenberg, A. R., Lassus, P., and Hibner, U. (2012) Hepatitis C viral protein NS5A induces EMT and participates in oncogenic transformation of primary hepatocyte precursors. *J Hepatol* **57**, 1021-1028
48. Elbirt, K. K., Whitmarsh, A. J., Davis, R. J., and Bonkovsky, H. L. (1998) Mechanism of sodium arsenite-mediated induction of heme oxygenase-1 in hepatoma cells. Role of mitogen-activated protein kinases. *The Journal of biological chemistry* **273**, 8922-8931
49. Kim, J. Y., Choi, J. A., Kim, T. H., Yoo, Y. D., Kim, J. I., Lee, Y. J., Yoo, S. Y., Cho, C. K., Lee, Y. S., and Lee, S. J. (2002) Involvement of p38 mitogen-activated protein kinase in the cell growth inhibition by sodium arsenite. *Journal of cellular physiology* **190**, 29-37
50. McKendrick, L., Morley, S. J., Pain, V. M., Jagus, R., and Joshi, B. (2001) Phosphorylation of eukaryotic initiation factor 4E (eIF4E) at Ser209 is not required for protein synthesis in vitro and in vivo. *European journal of biochemistry* **268**, 5375-5385
51. Bianchini, A., Loiarro, M., Bielli, P., Busà, R., Paronetto, M. P., Loreni, F., Geremia, R., and Sette, C. (2008) Phosphorylation of eIF4E by MNKs supports protein synthesis, cell cycle progression and proliferation in prostate cancer cells. *Carcinogenesis* **29**, 2279-2288
52. Grzmil, M., Morin, P., Jr., Lino, M. M., Merlo, A., Frank, S., Wang, Y., Moncayo, G., and Hemmings, B. A. (2011) MAP kinase-interacting kinase 1 regulates SMAD2-dependent TGF-beta signaling pathway in human glioblastoma. *Cancer research* **71**, 2392-2402
53. Baird, T. D., Palam, L. R., Fusakio, M. E., Willy, J. A., Davis, C. M., McClintick, J. N., Anthony, T. G., and Wek, R. C. (2014) Selective mRNA translation during eIF2 phosphorylation induces expression of IBTKα. *Molecular biology of the cell* **25**, 1686-1697
54. Romero, A. M., Ramos-Alonso, L., Alepuz, P., Puig, S., and Martinez-Pastor, M. T. (2020) Global translational repression induced by iron deficiency in yeast depends on the Gcn2/eIF2alpha pathway. *Scientific reports* **10**, 233
55. Muranen, T., Selfors, L. M., Worster, D. T., Iwanicki, M. P., Song, L., Morales, F. C., Gao, S., Mills, G. B., and Brugge, J. S. (2012) Inhibition of PI3K/mTOR leads to adaptive resistance in matrix-attached cancer cells. *Cancer cell* **21**, 227-239

649 56. Darling, N. J., and Cook, S. J. (2014) The role of MAPK signalling pathways in the response to
650 endoplasmic reticulum stress. *Biochimica et biophysica acta* **1843**, 2150-2163
651 57. Jiang, Q., Li, F., Shi, K., Wu, P., An, J., Yang, Y., and Xu, C. (2014) Involvement of p38 in signal
652 switching from autophagy to apoptosis via the PERK/eIF2α/ATF4 axis in selenite-treated NB4
653 cells. *Cell Death & Disease* **5**, e1270-e1270
654 58. Thiaville, M. M., Pan, Y. X., Gjymishka, A., Zhong, C., Kaufman, R. J., and Kilberg, M. S. (2008)
655 MEK signaling is required for phosphorylation of eIF2alpha following amino acid limitation of
656 HepG2 human hepatoma cells. *The Journal of biological chemistry* **283**, 10848-10857

657

658

659

660

661

662

663

664

665

666

667

668

669

670

671

672

673

674

675

676

677

678 Figure 1

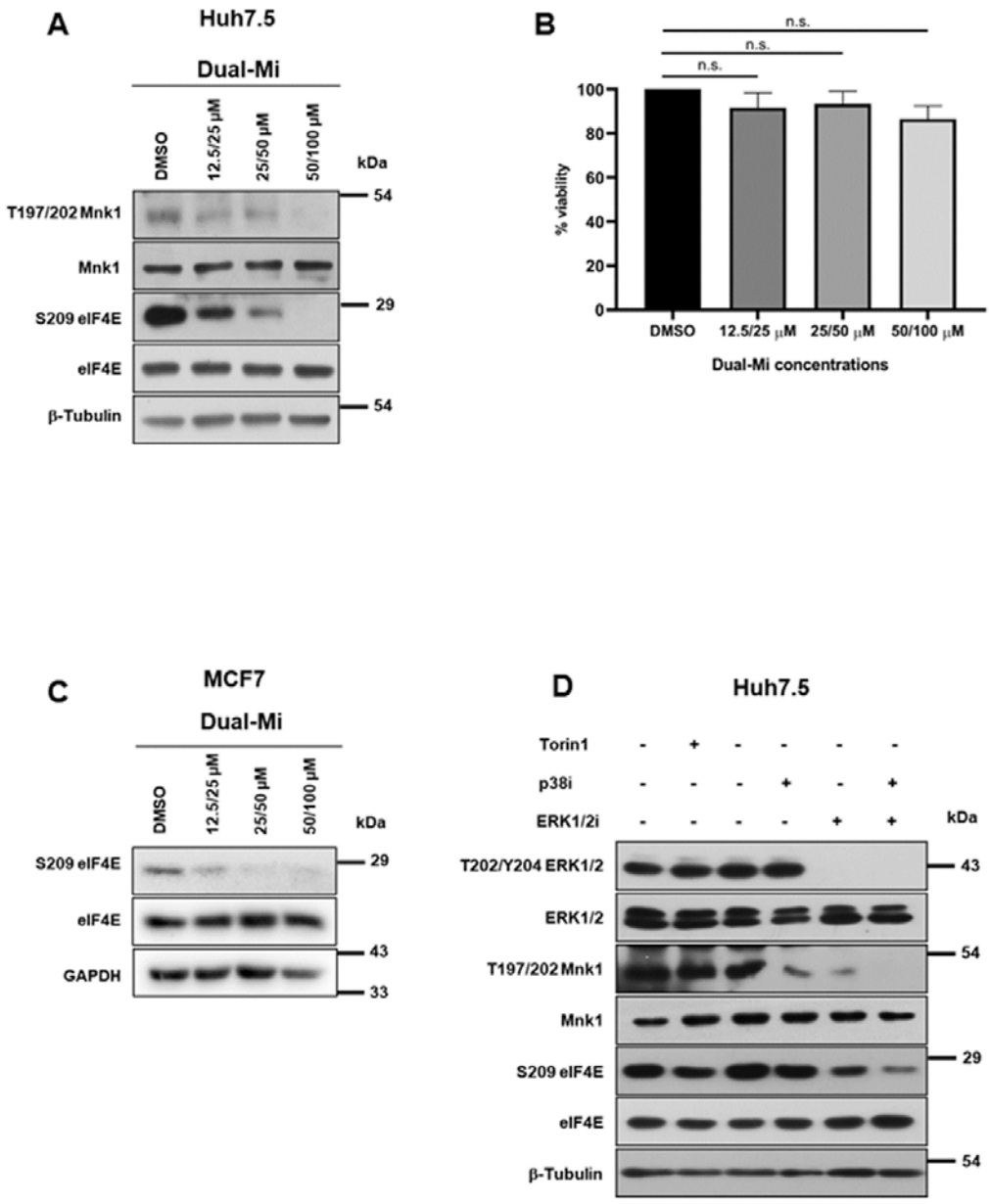

679

680

681

682

683

684

685 Figure 2

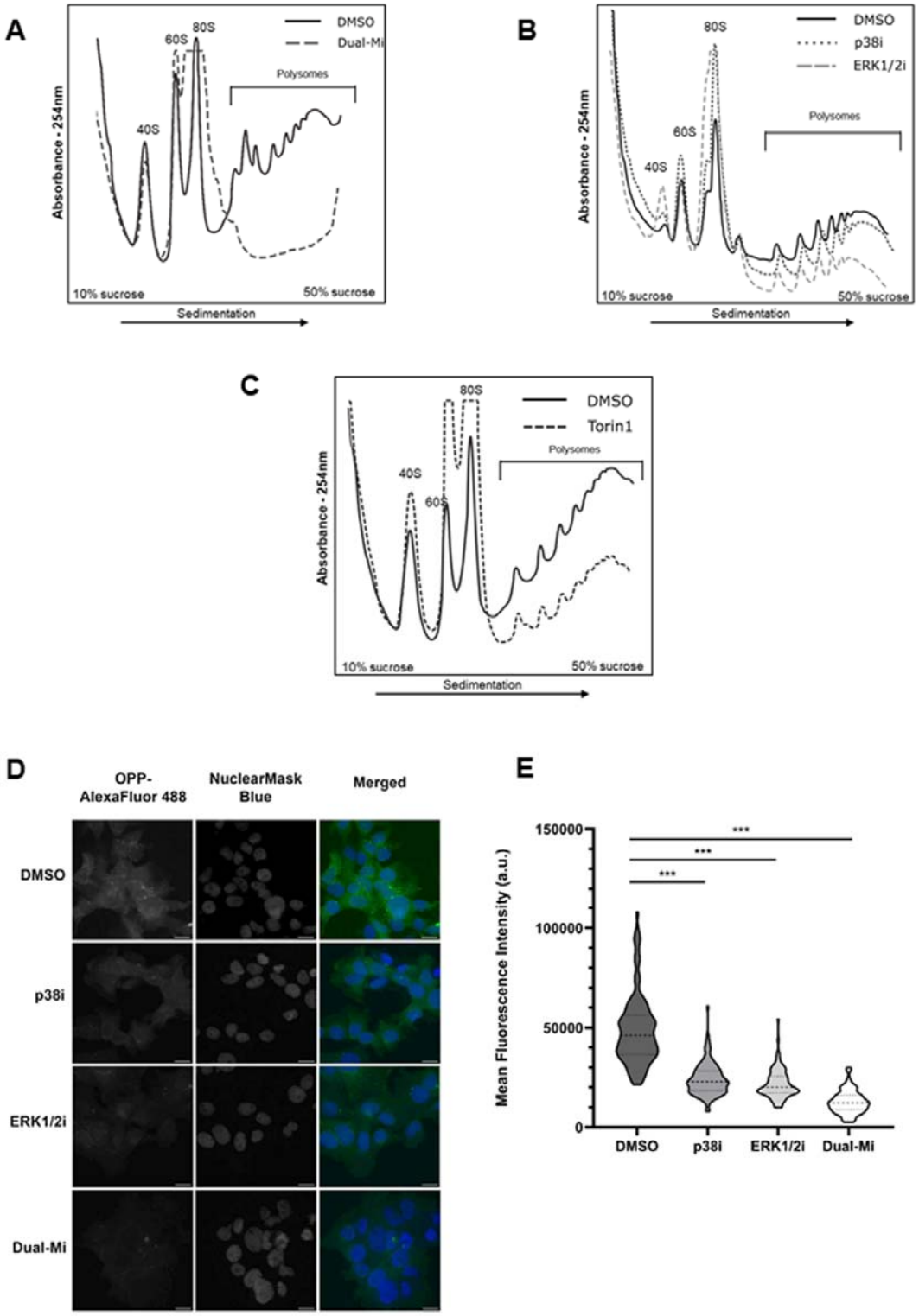

686

687

Figure 3

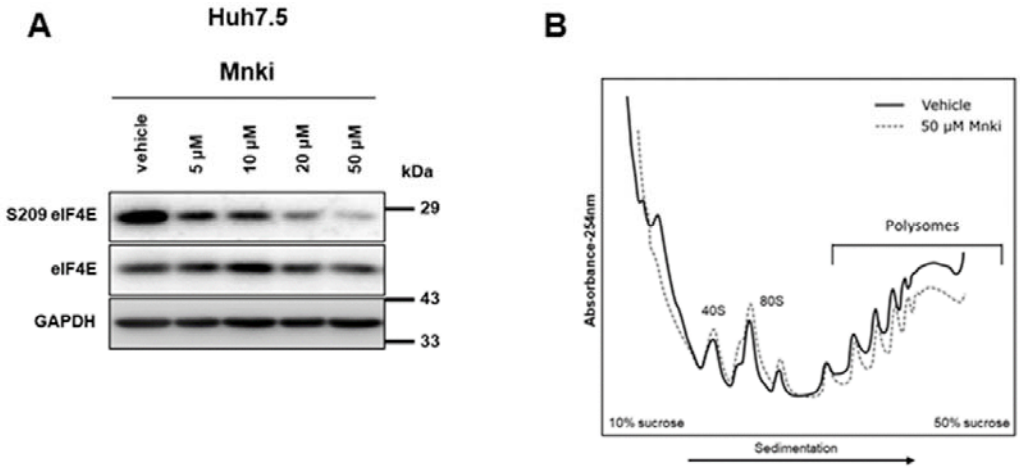

Figure 4

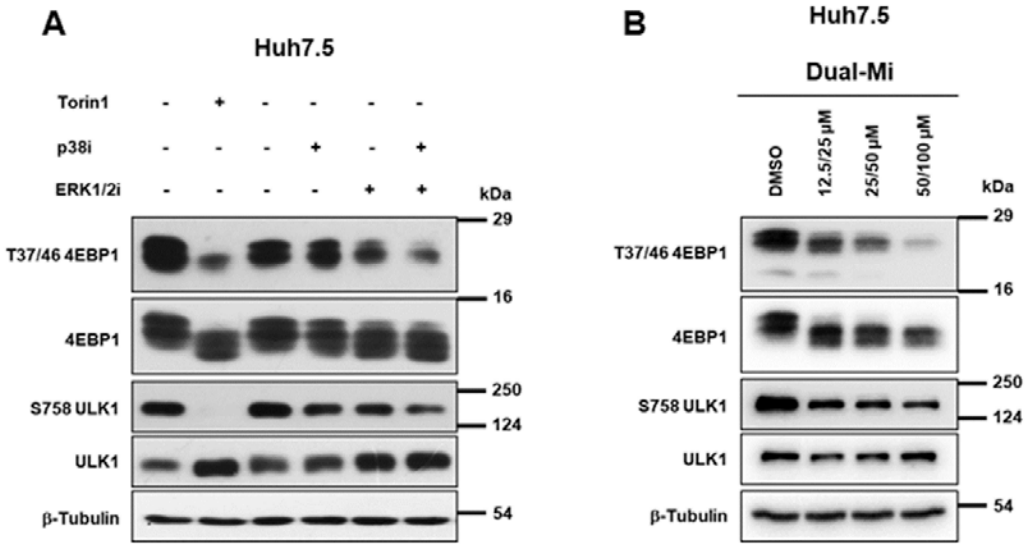

718 Figure 5

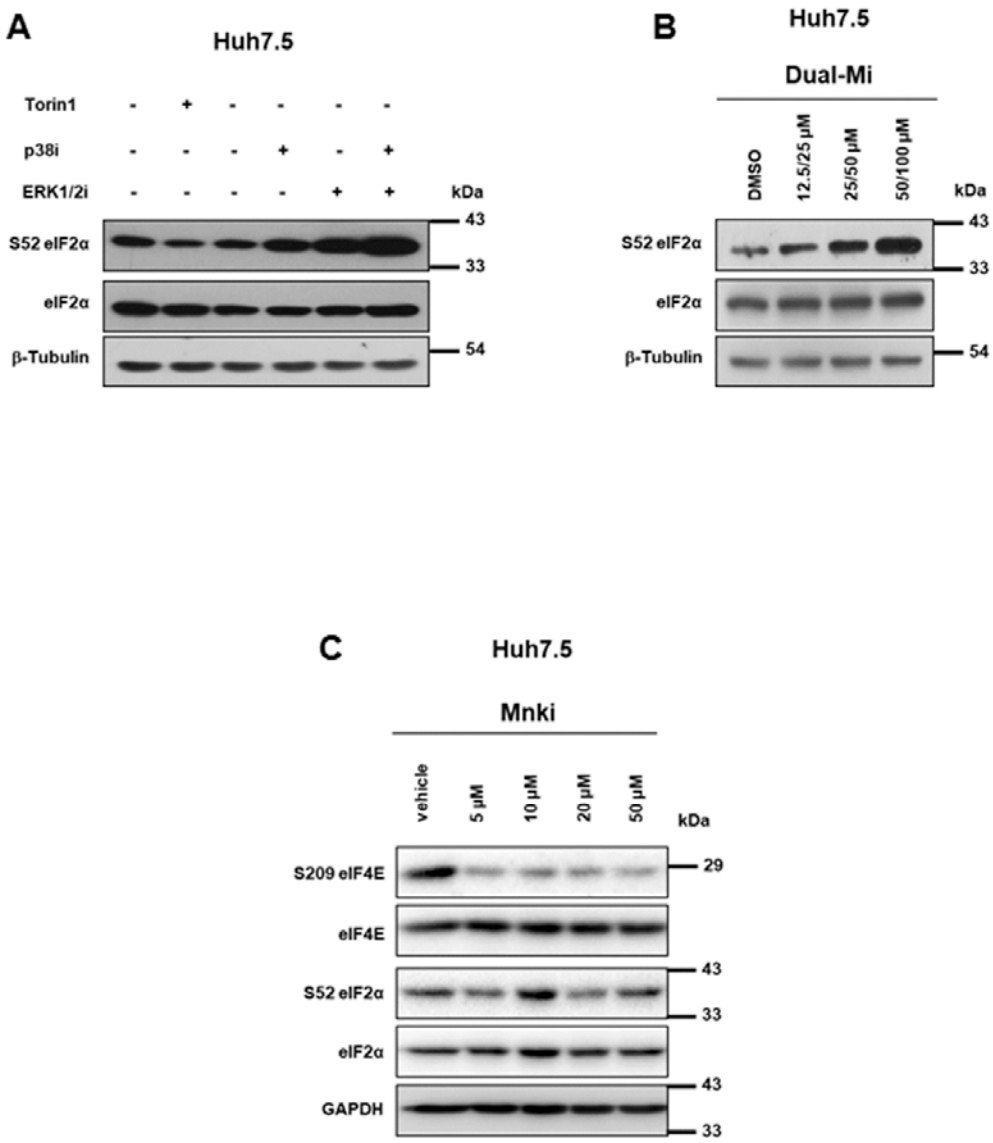

719

720

721

722

723

724

725 Figure 6

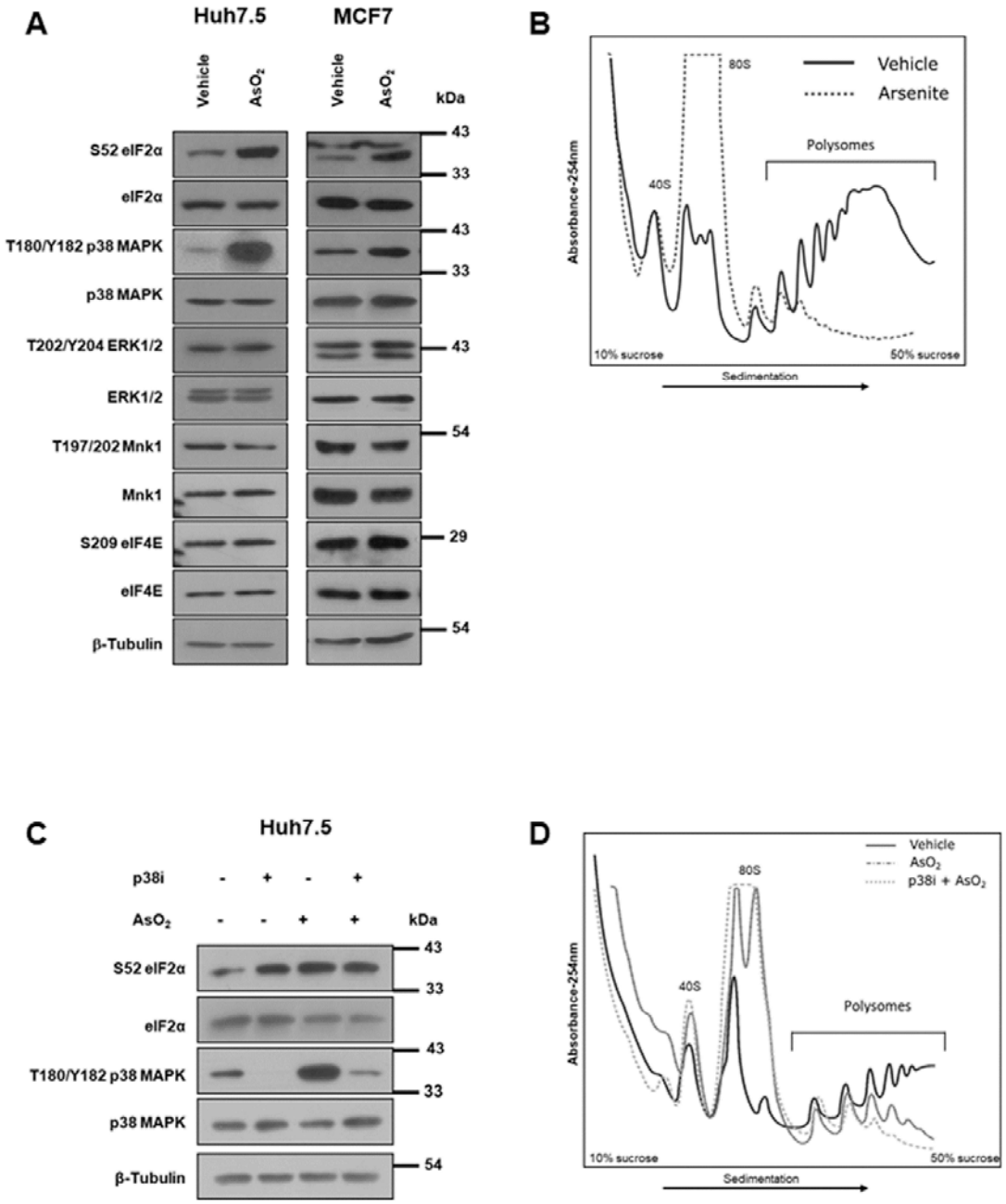

726

727

728

729

730 Figure 7

731

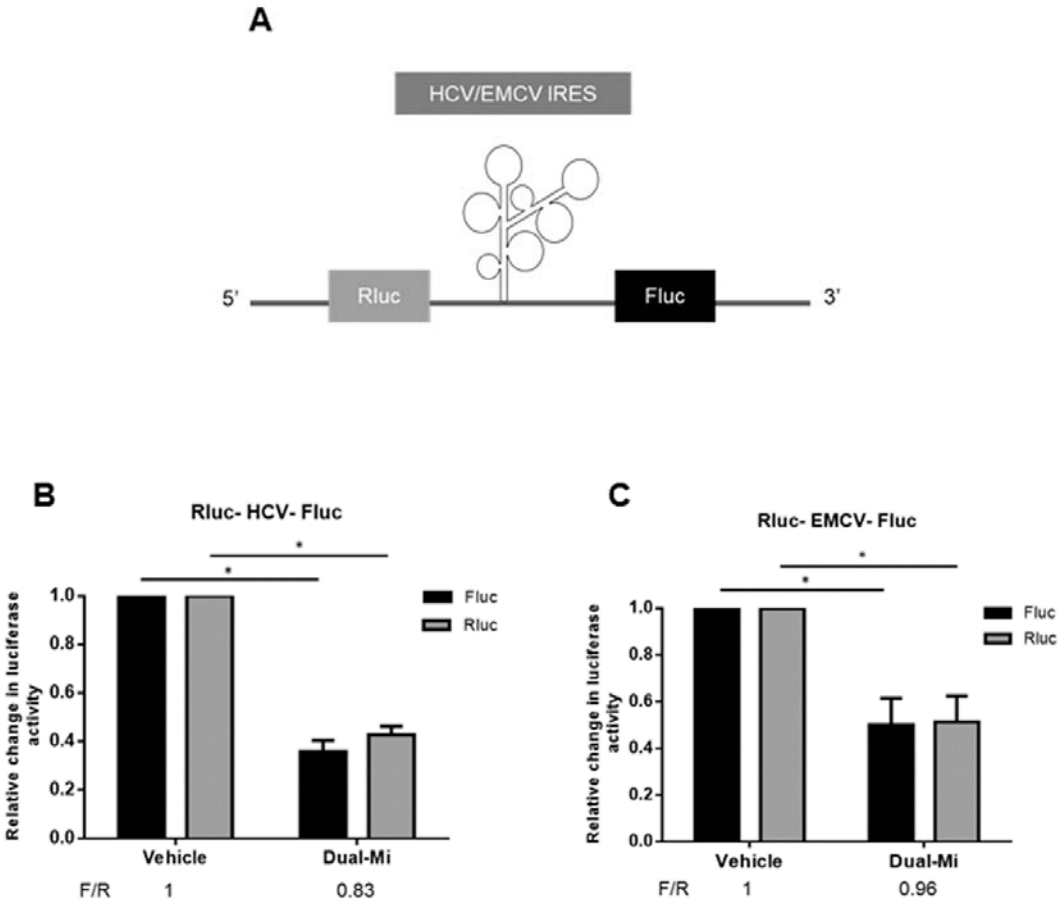

732

733 Figure 8

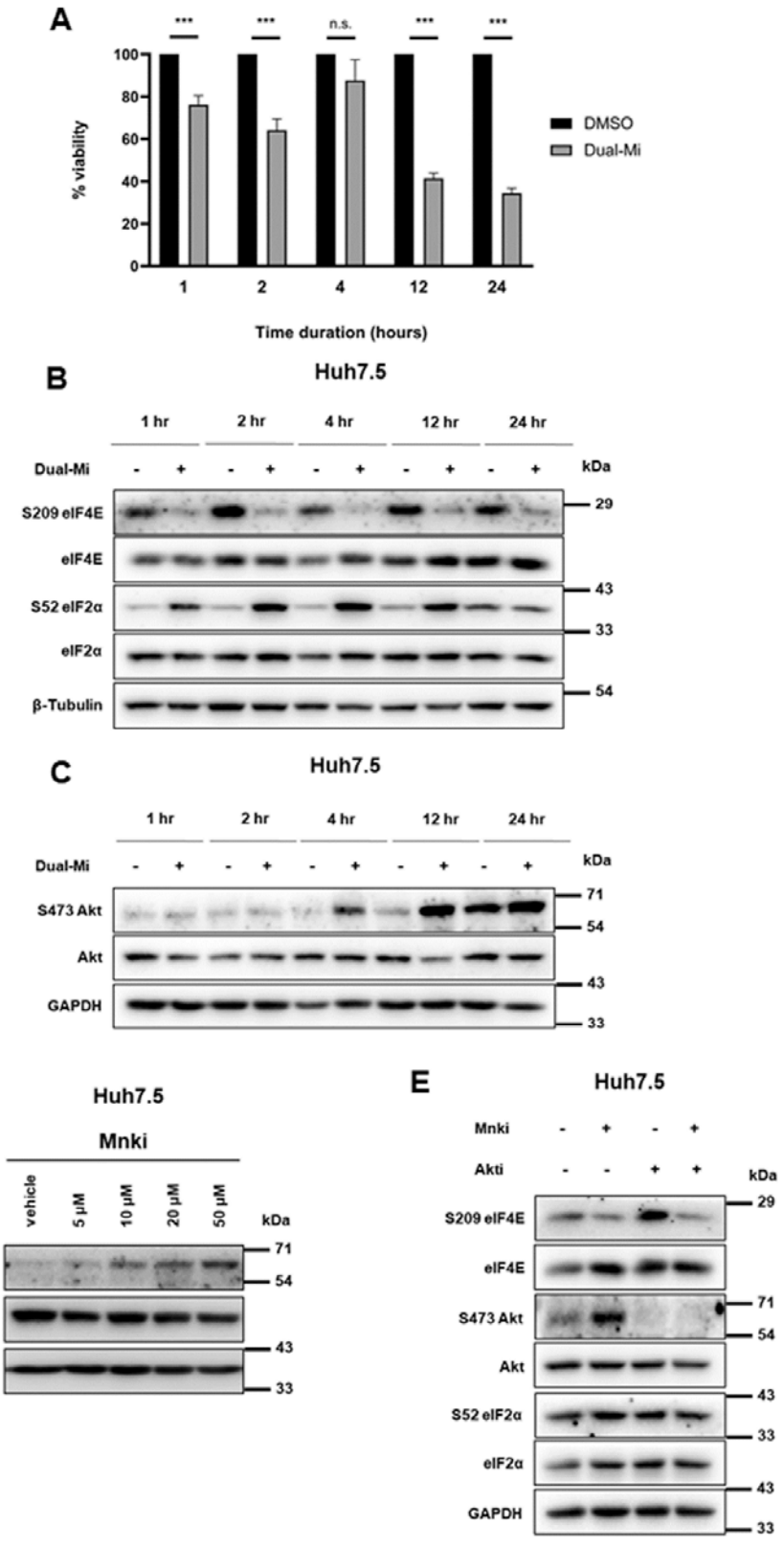

734

LEGENDS

Figure 1. p38 and ERK1/2 MAPK co-inhibition causes dose dependent decrease in eIF4E phosphorylation. (A) Immunoblots depicting phosphorylation and expression status of Mnk1 and eIF4E from Huh7.5 cells upon treatment with 12.5/25, 25/50, or 50/100 µM of dual-MAPK inhibitors (Dual-Mi) for 1- hour along with DMSO vehicle control. (**B)** Huh7.5 cell viability was measured upon treatment with DMSO vehicle or different concentrations of inhibitors for 1- hour using trypan blue exclusion method. Graph is representative of 3 independent experiments. The statistical significance was calculated using two tailed, paired Student's *t* test where n.s. represents non-significant. **(C)** Immunoblots depicting phosphorylation and expression of eIF4E from MCF7 cells upon similar treatment as in (A). **(D)** Immunoblots depicting phosphorylation and expression status of ERK1/2, Mnk1, and eIF4E from Huh7.5 cells treated with DMSO vehicle control, Torin1 (750 nM), p38i (50 µM), ERK1/2i (100 µM), or Dual-Mi (50/100 µM p38i/ERK1/2i). Lanes 1 and 3 are independent vehicle controls for Torin1 and MAPK inhibitors, respectively. p38i-p38 MAPK inhibitor VIII, ERK1/2i-U0126, Dual-Mi-p38i+ERK1/2i.

Figure 2. p38 and ERK1/2 MAPK dual inhibition severely affects polysome stability and suppresses translation. (A-C) Polysome profiles of Huh7.5 cells treated with DMSO vehicle control or specific inhibitor(s) for 1- hour. Polysome profile analyses were performed after density gradient ultracentrifugation of the corresponding cytosolic extract. Free ribosomal subunits (40S and 60S), monosome (80S) and the polyribosomes were fractionated by measuring the absorbance at 254 nm. Each graph shows treatment-curve overlaid on the vehicle control. **(A)** From dual-Mi (50/100 µM p38i/ERK1/2i) treatment. **(B)** From p38i (50 µM) and ERK1/2i (100 µM) individual treatments. **(C)** From Torin1 (750 nM) treatment. **(D)**

Representative images from OPP-incorporation assay for assessing protein synthesis in DMSO, p38i (50 µM), ERK1/2i (100 µM) and dual-Mi (50/100 µM p38i/ERK1/2i), performed in Huh7.5 cells. AlexaFluor 488 conjugated-OPP (green) was used to determine level of nascent protein synthesis. NuclearMask Blue (blue) was used to stain the nucleus. Images were captured at 20× magnification and the scale bar represents 20 µm length. **(E)** Quantitative analysis of OPP-incorporation depicted as violin plots. Data represented is from ~90 cells as 3 independent experimental setups and is represented with median values and minimum and maximum quartiles, and *p*-value was calculated using one-way ANOVA; *** represents $p < 0.0005$.

Figure 3. Polysome collapse caused by dual-Mi is independent of Mnk1/2 inhibition and eIF4E dephosphorylation. (A) Immunoblots depicting phosphorylation and expression status of eIF4E from Huh7.5 cells upon treatment with 5, 10, 20 or 50 µM of Mnki for 1- hour along with water vehicle control. (**B)** Polysome profiles from Huh7.5 cells upon treatment with vehicle or Mnki (50 µM) for 1- hour. Free ribosomal subunits (40S and 60S), monosome (80S) and the polysomes were fractionated by measuring the absorbance at 254 nm after density gradient centrifugation of corresponding cytosolic extracts. The graph shows treatment-curve overlaid on the vehicle. Mnki - ETP-45835

Figure 4. Dual-Mi causes moderate inhibition of mTORC1 activity in Huh7.5. (A) Immunoblots depicting phosphorylation and expression status of 4EBP1 and ULK1 from Huh7.5 cells treated with DMSO vehicle control, Torin1 (750 nM), p38i (50 µM), ERK1/2i (100 µM), or Dual-Mi (50/100 µM p38i/ERK1/2i) for 1- hour. (**B)** Immunoblot depicting phosphorylation and expression status of 4EBP1 and ULK1

784 from Huh7.5 cells upon treatment with 12.5/25, 25/50, or 50/100 µM of p38i/ERK1/2i
785 dual-MAPK inhibitors for 1- hour along with DMSO vehicle control.

786 **Figure 5. p38 and ERK1/2 MAPKs synergistically regulate eIF2α**
787 **phosphorylation independent of its common downstream kinase Mnk1/2. (A)**
788 Immunoblots depicting phosphorylation status of eIF2α from Huh7.5 cells treated
789 with DMSO vehicle control, Torin1 (750 nM), p38i (50 µM), ERK1/2i (100 µM) or
790 Dual-Mi (50/100 µM p38i /ERK1/2i) for 1- hour. **(B)** Immunoblots depicting
791 phosphorylation and expression status of eIF2α from Huh7.5 cells upon treatment
792 with 12.5/25, 25/50, or 50/100 µM of Dual-Mi for 1- hour along with DMSO vehicle
793 control. **(C)** Immunoblots depicting phosphorylation of eIF4E and eIF2α from Huh7.5
794 cells upon treatment with 5, 10, 20 or 50 µM of Mnki for 1- hour along with water
795 vehicle control.

796 **Figure 6. Arsenite induced p38 MAPK activation is critical for polysome**
797 **stability. (A)** Immunoblots depicting phosphorylation and expression status of eIF2α,
798 p38 MAPK, ERK1/2, Mnk1 and eIF4E from Huh7.5 and MCF7 cells upon treatment
799 with vehicle or sodium arsenite (40 µM) for 1- hour. **(B)** Polysome profiles from
800 Huh7.5 cells treated with vehicle or sodium arsenite (40 µM) for 1- hour. Free
801 ribosomal subunits (40S and 60S), monosome (80S) and the polyribosomes were
802 fractionated by measuring the absorbance at 254 nm after density gradient
803 centrifugation of corresponding cytosolic extracts. The graph shows treatment-curve
804 overlaid on that of the vehicle. **(C)** Immunoblots depicting phosphorylation and
805 expression status of eIF2α and p38 MAPK upon treatment with vehicle, sodium
806 arsenite (40 µM), p38i (50 µM) or both (40/50 µM sodium arsenite/p38i) for 1- hour.
807 **(D)** Polysome profiles from Huh7.5 cells treated with vehicle, sodium arsenite (40
808 µM), or both (40/50 µM sodium arsenite/p38i) for 1- hour. Free ribosomal subunits

(40S and 60S), monosome (80S) and the ribosomes were fractionated by measuring the absorbance at 254 nm after density gradient centrifugation of corresponding cytosolic extracts. The graph shows treatment-curve overlaid on the vehicle. AsO_2-Sodium arsenite.

Figure 7. Dual-Mi inhibits both cap-dependent and cap-independent translation. (A) Schematic representation of dual-luciferase reporter construct where HCV/EMCV IRES elements are sandwiched between *Renilla* (Rluc) and Firefly (Fluc) luciferase genes. (**B and C)** Luciferase assay in Huh7.5 lysates transfected with HCV **(B**) and EMCV **(C)** dual-luciferase reporter plasmids for 9-hours and further treatment either with vehicle or dual-Mi (50/100 µM p38i/ERK1/2i) for 1- hour. Relative change in luciferase activity was calculated by normalizing Fluc/Rluc reading of inhibitor treated cells with its corresponding vehicle control. *p*-value was calculated using two tailed, paired Student's *t*-test; * represents $p < 0.05$. F/R ratio of each treatment is represented below each graph.

Figure 8. Chronic inhibition of p38 and ERK1/2 MAPK results in activation of alternate cell survival pathways to support cell sustenance. (A) Viability of Huh7.5 cells upon treatment with DMSO vehicle control or dual-Mi (50/100 µM p38i/ERK1/2i) for 1-, 2-, 4-, 12- or 24- hours using MTT assay. Graph is representative of three independent experiments. *p*-value was calculated using two tailed, paired Student's *t*-test; where *** represents $p < 0.0005$ and n.s. represents non-significant. **(B)** Immunoblots depicting phosphorylation and expression status of eIF2α, eIF4E from Huh7.5 cells upon treatment with DMSO vehicle control or dual-Mi (50/100 µM p38i/ERK1/2i) for 1-, 2-, 4-, 12- or 24- hours. **(C)** Those of Akt from the same treatment as in (B). **(D)** Immunoblots depicting phosphorylation and expression status of Akt from Huh7.5 cells upon treatment with 5, 10, 20 or 50 µM of Mnki for 1

hour along with water vehicle control. **(E)** Immunoblots depicting phosphorylation and expression status of eIF4E, Akt and eIF2α from Huh7.5 cells upon treatment with vehicle, Mnki (10 µM), Akti (5 µM) or both (10/5 µM Mnki/Akti), Akti-Akt inhibitor VIII.

Supplementary information

Figure S1

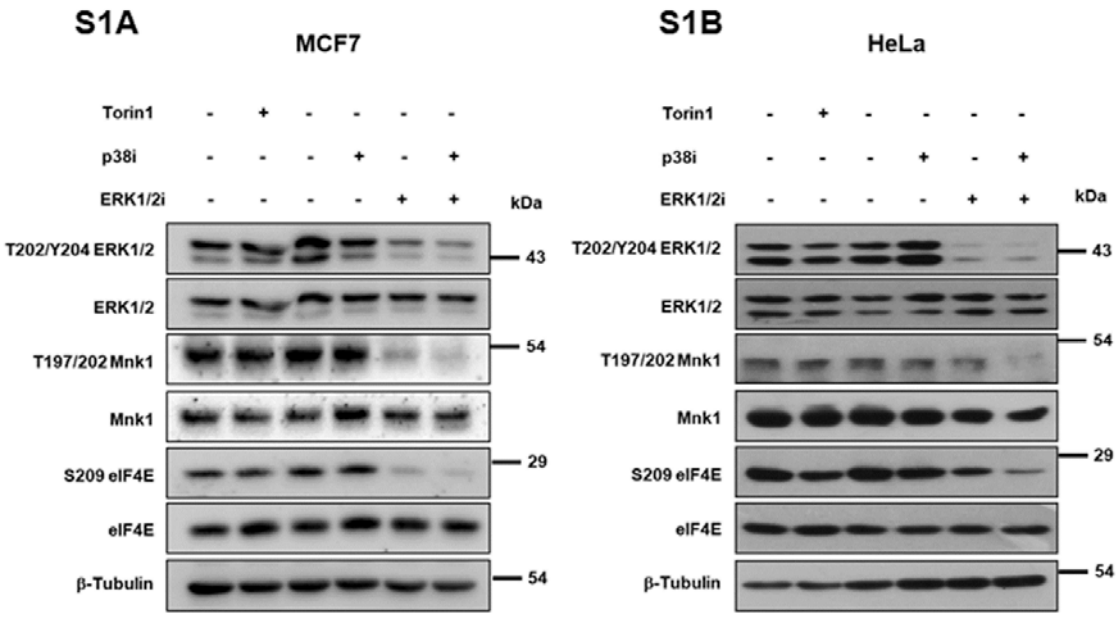

Supplementary Figure S1. p38 and ERK1/2 MAPK synergistically regulates eIF4E phosphorylation across multiple cell lines. (S1A) Immunoblots depicting phosphorylation and expression status of ERK1/2, Mnk1 and eIF4E from MCF7 cells treated with DMSO vehicle control, Torin1 (750 nM), p38i (50 µM), ERK1/2i (100 µM) or Dual-Mi (50/100 µM p38i/ERK1/2i). **(S1B)** Immunoblots depicting phosphorylation and expression status of ERK1/2, Mnk1, and eIF4E from HeLa cells treated as mentioned in (S1A).

Figure S2

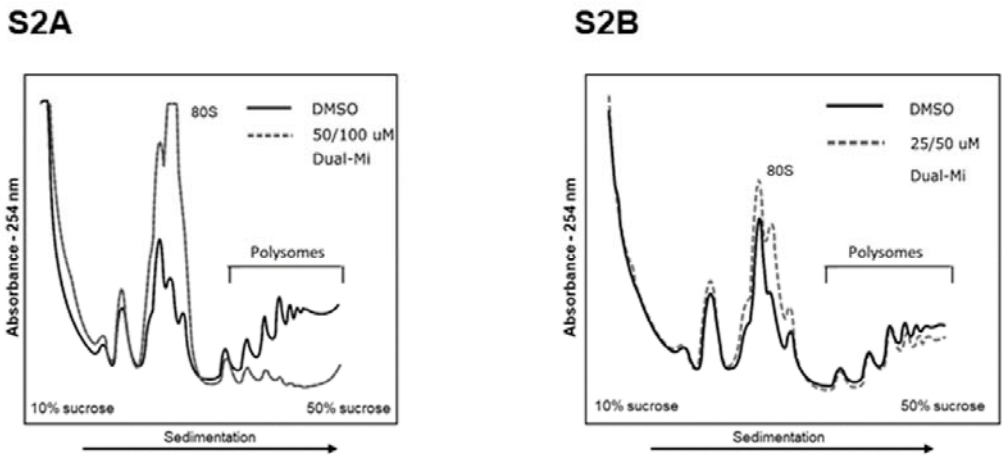

Supplementary Figure S2. p38 and ERK1/2 dual inhibition causes polysomal collapse in MCF7 cells. (S2A) MCF7 cells were subjected to dual-Mi (50/100 µM p38i/ERK1/2i) or to DMSO treatment for 1- hour and polysome profiling was performed. (**S2B**) Polysome profile of the cells subjected to similar treatment but at lower concentrations of the inhibitors (25/50 µM p38i/ERK1/2i). Free ribosomal subunits (40S and 60S), monosome (80S) and the polysomes were fractionated by measuring the absorbance at 254 nm. Each graph shows treatment-curve overlaid on the vehicle control.

Figure S3

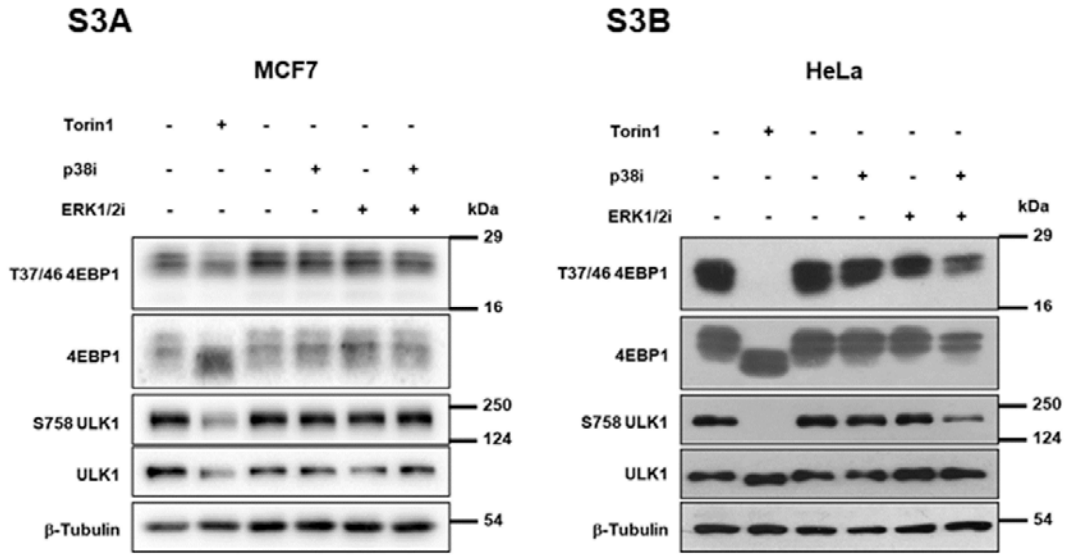

Supplementary Figure S3. Regulation of mTORC1 pathway by p38 and ERK1/2 MAPKs is contextual. (S3A) Immunoblots depicting phosphorylation and expression status of 4EBP1 and ULK1 from MCF7 cells treated with DMSO vehicle control, Torin1 (750 nM), p38i (50 μM), ERK1/2i (100 μM) or Dual-Mi (50/100 μM p38i/ERK1/2i) for 1- hour. **(S3B)** Immunoblots demonstrating phosphorylation and expression status of 4EBP1 and ULK1 from HeLa cells treated with DMSO vehicle control, Torin1 (750 nM), p38i (50 μM), ERK1/2i (100 μM) or Dual-Mi (50/100 μM p38i/ERK1/2i) for 1- hour.

905 Figure S4

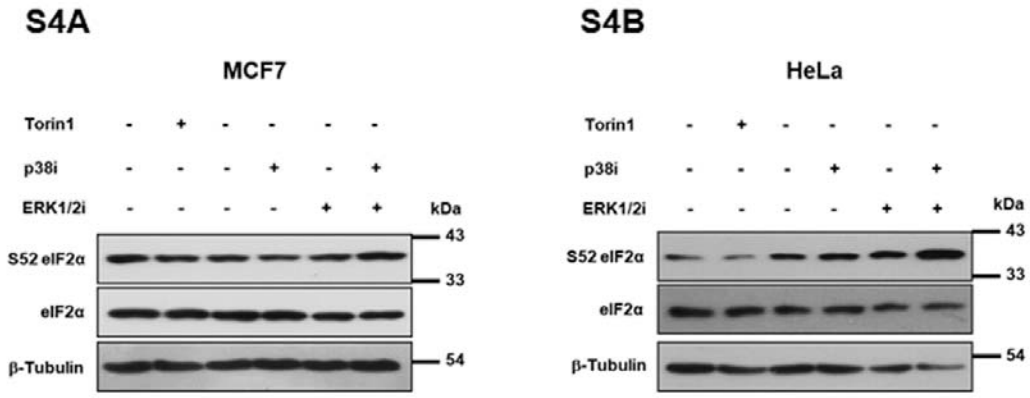

906

907

908 **Supplementary Figure S4. p38 and ERK1/2 dual-MAPK inhibition activates ISR**

909 **signalling. (S4A)** Immunoblots depicting phosphorylation and expression status of

910 eIF2α from MCF7 cells treated with DMSO vehicle control, Torin1 (750 nM), p38i (50

911 μM), ERK1/2i (50 μM) or Dual-Mi (50/50 μM p38i/ERK1/2i) for 1- hour. **(S4B)**

912 Immunoblots depicting phosphorylation status of eIF2α from HeLa cells treated with

913 DMSO vehicle control, Torin1 (750 nM), p38i (50 μM), ERK1/2i (100 μM) or Dual-Mi

914 (50/100 μM p38i/ERK1/2i) for 1- hour.

915

916

917

918

919

920

921

922 Figure S5

923

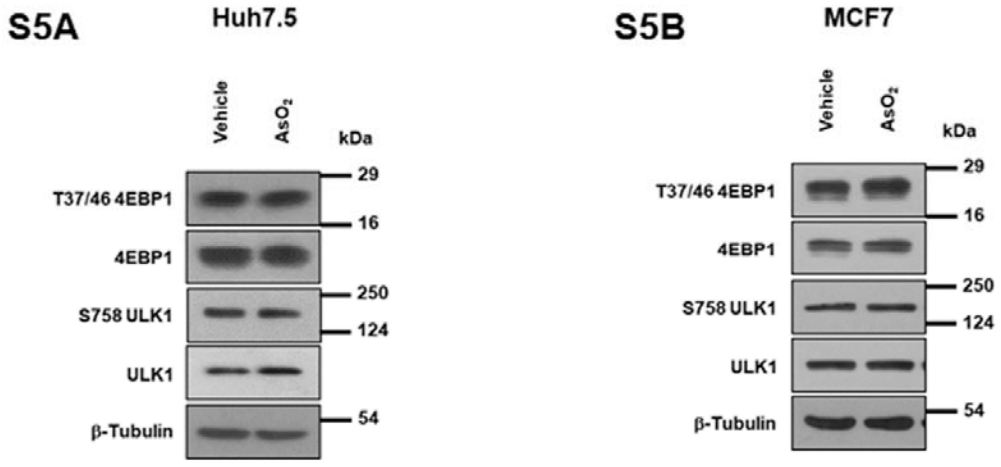

924

925

926 **Supplementary Figure S5 mTORC1 pathway was unaffected during sodium**

927 **arsenite induced ISR. (S5A)** Immunoblots depicting phosphorylation and

928 expression status of 4EBP1 and ULK1 from vehicle or sodium arsenite (40 µM)

929 treated Huh7.5 cells for 1- hour. **(S5B)** Immunoblots depicting phosphorylation and

930 expression status of 4EBP1 and ULK1 from vehicle or sodium arsenite (40 µM)

931 treated MCF7 cells for 1- hour.

932

933